RinginRing Assembly Facilitates the Synthesis of a [12]Cycloparaphenylene ABCType [3]Catenane

Ring-in-Ring Assembly Facilitates the Synthesis of a Cycloparaphenylene ABC-Type [3]Catenane

Wudi Shi,[a] Yaning Hu,[a] Luigi Leanza,[b] Yevhenii Shchukin,[c] Patrick A. Hoffmann,[c] Menghua Li,[a] Chengbing Ning,[a] Zhong-Yan Cao,[a] Yuanqing Xu,[a] Pingwu Du,[d,*] Max von Delius,[c,*] Giovanni M. Pavan,[b,*] Youzhi Xu[a,*]

[a] College of Chemistry and Molecular Sciences, Henan University, Kaifeng 475004, China

[b] Department of Applied Science and Technology, Politecnico di Torino, Corso Duca degli Abruzzi, 24, 10129 Torino, Italy

[c] Institute of Organic Chemistry, Ulm University, Albert-Einstein-Allee 11, 89081 Ulm, Germany

[d] Hefei National Laboratory for Physical Sciences at the Microscale, CAS Key Laboratory of Materials for Energy Conversion, Department of Materials Science and Engineering, University of Science and Technology of China, Hefei, Anhui Province, 230026 China.

KEYWORDS: *Cycloparaphenylene; [3]Catenane; Ring-in-Ring Assembly; Mechanically Interlocked Molecules; Molecular Dynamics*

ABSTRACT: Cycloparaphenylenes (CPPs) represent a significant challenge for the synthesis of mechanically interlocked architectures, because they lack heteroatoms, which precludes traditional active and passive template methods. To circumvent this problem and explore the fundamental and functional properties of CPP rotaxanes and catenanes, researches have resorted to unusual non-covalent and even to labor-intensive covalent template approaches. Herein, we report a ring-in-ring non-covalent template strategy that makes use of the surprisingly strong non-covalent inclusion of crown ethers into suitably sized CPPs. By threading a secondary ammonium salt through the crown ether and closing the third ring via CuAAC click reaction, we obtained a rare ABC-type hetero-[3]catenane comprising [12]CPP, 24-crown-8 and a dibenzylammonium macrocycle. X-ray crystallography shed light on the ring-in-ring pre-organization and the [3]catenane topology was confirmed by NMR and MS-MS studies. Molecular simulations provided insights into the intriguing ring-vs.-ring-vs.-ring dynamics of the [3]catenane, which are highly dependent on the protonation state of the dibenzylammonium site. This ring-in-ring assembly strategy opens new avenues for the synthesis of complex CPP architectures and their use in functional supramolecular systems.

INTRODUCTION

Mechanically interlocked molecules (MIMs) are composed of two or more molecular units linked not by traditional chemical bonds, but as a consequence of specific molecular topology that includes several "crossing points". Classic examples of rotaxanes, catenanes, and molecular knots.[1] Because MIMs contain components that are not connected via rigid covalent bonds, the relative position of the components is typically highly dynamic, which has been used in applications across diverse fields, including molecular machinery, catalysis, and drug delivery systems.[2-8] Typically, the assembly of MIMs involves non-covalent interactions such as metal coordination,[9-12] hydrogen bonding,[13, 14] π–π interactions,[15] and electrostatic forces.[16] Prominent examples of these methods include pairing crown ethers with ammonium derivatives,[17-19] interactions between the electron-rich cavities of pillararenes and electron-deficient small molecules,[20-23] and the assembly of cyclobis(paraquat-*p*-phenylene) with viologen radicals to form mechanical bonds.[24-26] The very first rational synthesis of a [2]catenane was achieved by a tour de force covalent template approach.[27] [3]Catenanes featuring two different macrocycles (ABA-type) are hard to prepare,[28-30] but have nevertheless been employed in some of the most spectacular artificial molecular machines[31-33] reported to date. The rational synthesis of ABC-type hetero[3]catenanes or hetero[*n*]catenanes ($n>3$) is even more difficult, which is why examples are still scarce (Figure 1b).[34-38]

Strained carbon nanohoops, featuring radially uninterrupted π-conjugation such as [*n*]cycloparaphenylenes ([*n*]CPPs) and their derivatives, exhibit unique properties such as a size-dependent band gap.[39-42] Since their first synthesis in 2008, these molecules

have garnered significant research interest, initially for their potential as seed molecules in the bottom-up synthesis of carbon nanotubes[43] and increasingly for applications in supramolecular chemistry,[44, 45] catalysis[46] and organic electronics.[47-49] The structure of prototypical CPPs is characterized by large rigid cavities and lacks sites for metal coordination or hydrogen bonding. It therefore took ten years after their first report for prototypical CPPs to be integrated into MIMs via the concave–convex π–π interactions with a fullerene (Figure 1a).[50, 51] Heteroatom-containing CPPs have been used to construct MIMs based on efficient metal template and active metal template approaches (Figure 1).[52-56] Itami and Cong recently employed covalent template approaches to prepare MIMs comprising unaltered CPPs[57-59], while Ide, Tsuchido and coworkers reported a valuable method that makes use of non-covalent interactions, but is limited to the dodecamethoxy derivative of [6]CPP (Figure 1a).[60]

We were inspired by Jiang and coworkers recent demonstration that a [12]CPP derivative can form a supramolecular inclusion complex with 18-crown-6, facilitated by dispersion forces and multiple C–H···π interactions.[61] Specifically, we wondered whether a new type of [3]catenane could be made via ring-in-ring assembly involving the commercially available macrocycles [12]CPP and 24-crown-8 (Figure 1c). Here we show that such an ABC-type hetero[3]catenane can be prepared in up to 35% yield and report preliminary data on the relative dynamics of the three rings.

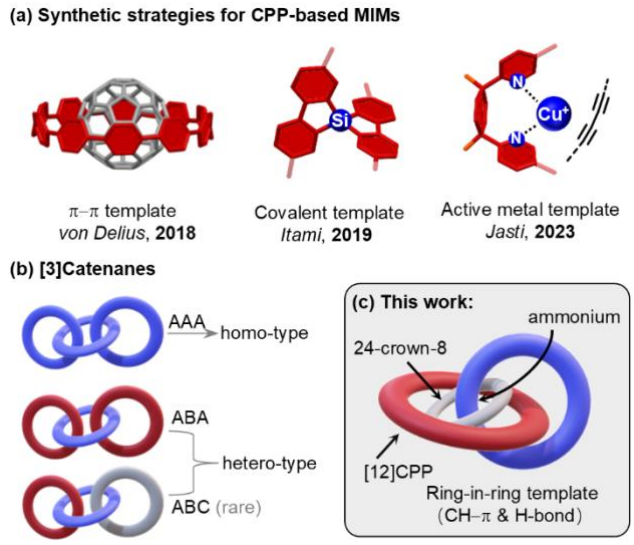

Figure 1. (a) Overview of previous strategies for the preparation of CPP-based MIMs. (b) Illustration of three fundamental types of [3]catenanes. (c) ABC-type topology described in this work and non-covalent interactions allowing ring-in-ring assembly.

RESULTS AND DISCUSSION

Synthesis Strategy and Preparation of Precursors. Constructing MIMs via a ring-in-ring assembly strategy necessitates considering the two rings and their binding affinities with the thread simultaneously. Although a moderate binding affinity is reported for the combination of a [12]CPP derivative and 18-crown-6,[61] the size of 18-crown-6 is evidently too small for axle molecules containing aryl groups. After investigating 18-crown-6 and 21-crown-7, we ultimately selected 24-crown-8 as the inner ring that serves to connect [12]CPP and the dibenzylammonium thread. Given that [12]CPP features a rigid cavity with a diameter of ca. 17 Å, only unusually large stoppers would be suitable for the preparation of a [3]rotaxane.[62] We therefore aimed to demonstrate our ring-in-ring assembly strategy for the synthesis of a [3]catenane. The essential building blocks [12]CPP (**3**), dibenzylammonium thread (**7**) and 24-crown-8 (**8**) required for the assembly of the target catenane can be purchased or synthesized following simple literature procedures (Figure 2a). In a Suzuki–Miyaura reaction, aryl dibromide **1** was coupled with aryl diboronic esters **2**, and a subsequent reductive aromatization gave [12]CPP in a two-step yield of 18%. Thread **7** features terminal alkyne and azide groups, enabling effective cyclization via the copper(I)-catalyzed azide-alkyne cycloaddition (CuAAC). To maximize the yield of intramolecular ring closure, we introduced two twelve-carbon alkyl chains on both sides of the aryl group.

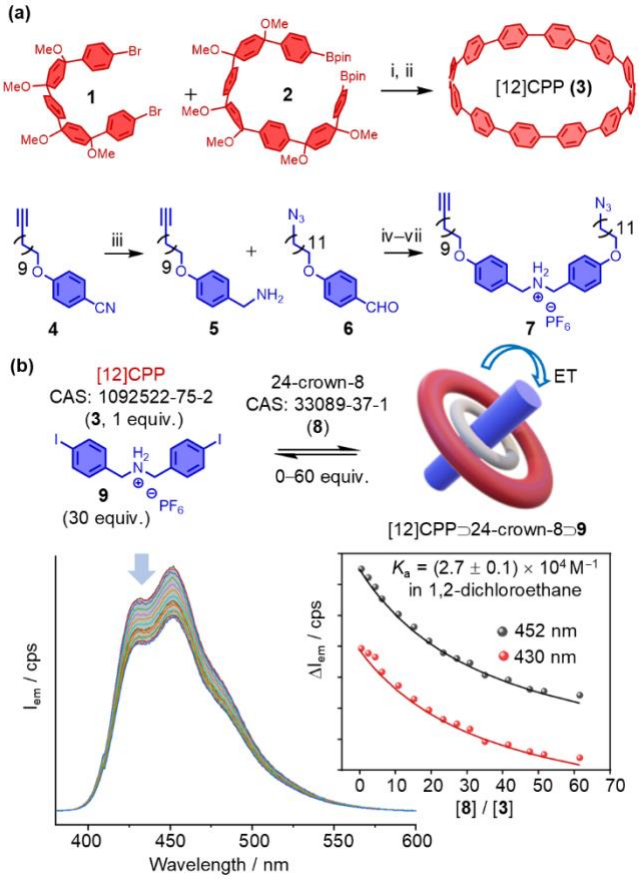

Figure 2. (a) Molecular structures and synthesis of key precursors. Reaction conditions: (i) K_3PO_4, 1,4-dioxane, dppf Pd G4, 85 °C, 24 h. (ii) Sodium naphthalenide, THF, −78 °C, 2 h, 18% (two-step yield). (iii) $LiAlH_4$, THF, 60 °C, 12 h, 80%. (iv) Toluene, 4 Å molecular sieves. (v) $NaBH_4$, MeOH, RT, 2 h, 80%. (vi) HCl 1M, MeOH. (vii) NH_4PF_6, 2 h. (b) Fluorescence titration between [12]CPP (conc. 1.0 × 10⁻⁶ M) and **9** (conc. range 0–6.1 × 10⁻⁵ M) in 1,2-dichloroethane. ET: electron transfer.

With the three key building blocks in hand, we attempted to evaluate the non-covalent association properties of ternary complex [12]CPP⊃24-crown-8⊃**7**. Unfortunately,

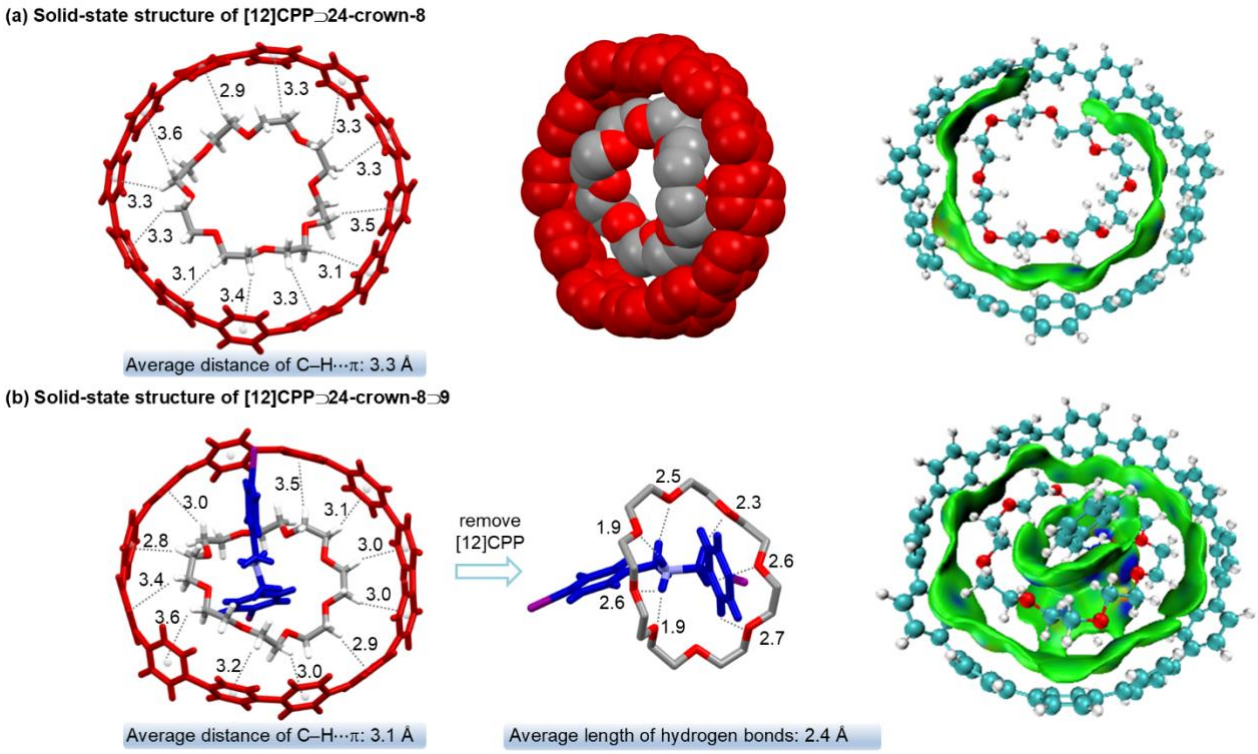

Figure 3. (a) X-ray crystal structure of the ring-in-ring complex [12]CPP⊃24-crown-8 and IGM analysis of the binary complex (δg_{inter} = 0.003). (b) X-ray crystal structure of the three-shell supramolecular complex [12]CPP⊃24-crown-8⊃**9** and IGM analysis of the ternary complex (δg_{inter} = 0.003).

neither ^{1}H NMR nor optical titration experiments were suited to obtain association constants. Therefore, we designed a simpler ternary model complex, in which we replaced the long side chains of the dibenzylammonium thread **7** with two heavy iodine atoms. The introduction of iodine in **9** allowed us to investigate the association by means of fluorescence quenching titrations. To study the three-shell complex[63, 64] via spectroscopic titration in 1,2-dichloroethane, we adopted an approximation previously used for similar three-component systems.[26, 65] In the presence of a large excess of **9** (30 equiv), the isotherm representing the binding of the two rings could be fitted relatively well with a 1:1 model, giving an apparent K_a of 2.7± 0.1 × 10^4 M^{-1}. When compared to the binary binding constant determined in the absence of **9** ($K_a = 5.5 \pm 0.3 \times 10^3$ M^{-1}, Figure S1), this result indicates that the dibenzylammonium guest promotes the supramolecular interactions of [12]CPP and 24-crown-8.

The favourable thermodynamics of the ternary complex [12]CPP⊃24-crown-8⊃**9** prompted us to grow single crystals by slow diffusion of *n*-hexane into a 1,2-dichloroethane solution of the complex (concentration: 0.05 M). Interestingly, both [12]CPP⊃24-crown-8 and [12]CPP⊃24-crown-8⊃**9** coexisted in a single unit cell simultaneously (Figure 3, Figure S2). Crystal structure analysis revealed that 24-crown-8 is perfectly encapsulated by [12]CPP, with an average distance of 3.3 Å between crown ether hydrogen atoms and the center CPP phenylene units (Figure 3a). In the ternary complex, the distance between [12]CPP and 24-crown-8 decreases further to approximately 3.1 Å, which is presumably due to an electrostatic enforcement of the multiple C–H···π interactions and would explain the observed cooperativity during self-assembly. The crystal structure of the ternary complex also shows that 24-crown-8 and **9** engage in strong non-covalent interactions through multiple hydrogen bonds, with an average O···H hydrogen bond distance of approximately 2.4 Å (Figure 3b). Independent gradient model (IGM) analyses further indicate that the ternary [12]CPP⊃24-crown-8⊃**9** complex exhibits stronger dispersion forces compared to the binary [12]CPP⊃24-crown-8 complex.

Catenane Synthesis and Characterization. Before evaluating the effectiveness of using a ring-in-ring approach to create MIMs, we explored the reaction conditions that should facilitate an efficient intramolecular CuAAC while not leading to disassembly of the ternary complex. (Figure 4a). In degassed dichloromethane, a 0.002 M solution of thread **7** undergoes an intramolecular click reaction to yield macrocycle **A** in 56% yield, catalyzed by $[Cu(CH_3CN)_4]PF_6$ in the presence of tris((1-benzyl-4-triazolyl)methyl)amine (TBTA; Figure 4a: *Route I*). Subsequently, we assessed the potential of this method to form catenanes in the presence of macrocycles 24-crown-8 and [12]CPP, respectively. After stirring 0.002 M of thread **7** with 2 equiv. of 24-crown-8 at room temperature for 8 hours, the addition of 10 mol% of $[Cu(CH_3CN)_4]PF_6$ followed by additional 8 hours reaction time furnished [2]catenane **B** in 41% yield (*Route II*).

However, when replacing the crown ether with [12]CPP (*Route III*), no [2]catenane was observed after carrying out the same procedure (*Route III*). Encouraged by these findings,

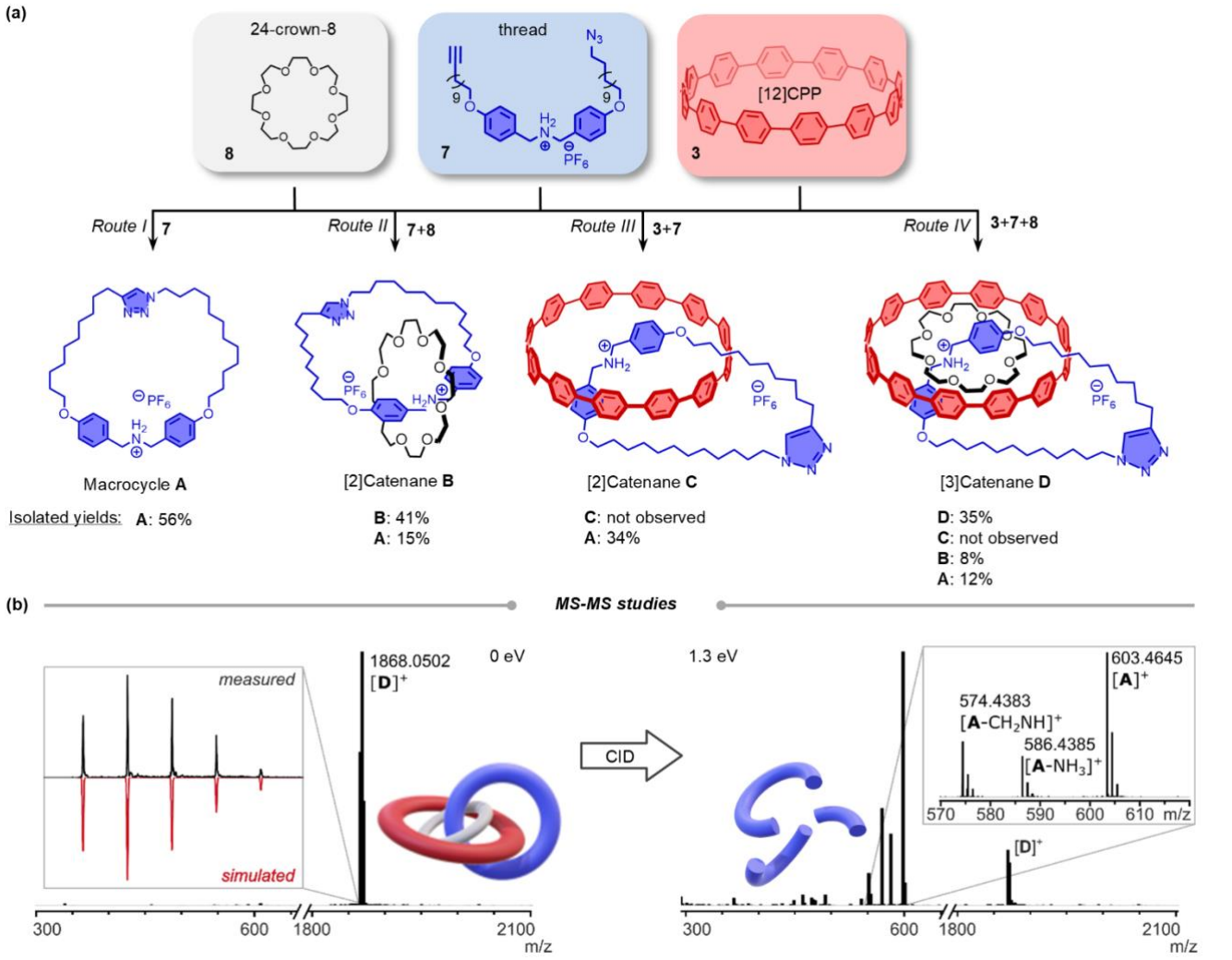

Figure 4. (a) Two types of catenanes formed from three simple components by CuAAC: $[Cu(CH_3CN)_4]PF_6$, TBTA, DCM, RT. (b) ESI^+ mass spectrum with inset of measured and simulated isotope pattern of catenane (**D**) (left). MS-MS spectrum of the catenane (**D**) (right), displaying the characteristic collision-induced dissociation (CID) behavior similar to catenane (**B**) and macrocycle (**A**). Due to the absence of charge, structures **8** and **3** could not be observed following the collision.

we attempted the synthesis of [3]catenane **D** via ring-in-ring assembly (Figure 4: *Route IV*). In degassed dichloromethane, a mixture containing 0.001 M of thread **7**, 1 equiv of [12]CPP, and 2 equiv. of 24-crown-8 was stirred overnight for pre-assembly. The following day, 10 mol% of $[Cu(CH_3CN)_4]PF_6$ was added, and stirring continued for 12 hours at room temperature, after which the product mixture was separated by preparative thin layer chromatography (TLC). To our delight, we obtained the [3]catenane **D** in 35% isolated yield. Besides the main product we obtained 12% of [2]catenane **B** along with a minor quantity of macrocycle **A** (8% yield) and recovered approximately 10% of the [12]CPP nanohoop. Moreover, a mixture of highly polar substances exhibiting bright luminescence similar to [12]CPP was observed, which could be indicative of oligocatenane formation.

The structures of **A**, **B** and **D** were fully characterized by NMR spectroscopy and high-resolution mass spectrometry (HRMS). Given the molecular weight of 1.8 kDa and the presence of two flexible macrocycles, it is not surprising that our attempts at growing single crystals of **D** suitable for X-ray crystallography were unsuccessful. Consequently, MS-MS experiments were carried out to provide evidence supporting the [3]catenane structure of **D**. Macrocycle **A** and two catenanes (**B** and **D**) were fragmented under varying collision energies. The survival yield curves of catenanes **B** and **D** were comparable to the one of macrocycle **A** (Figure S3), which strongly suggests that these compounds are not simple non-covalent adducts, but require the breaking of covalent bonds for their dissociation. Moreover, the characteristic fragmentation patterns which we observed in the MS-MS spectra of **A** (Figure S4, S5) were also found in catenanes **B** and **D** (Figure 4b and Figures S6, S7). This finding supports the [2]catenane topology for **B** and the [3]catenane topology for **D**, because these catenanes simply fall apart into the neutral macrocycles **3** and **8** upon cleavage of a bond in charged macrocycle **A**, which is the weakest link under the conditions of the CID experiments.

The ^{1}H NMR spectra of [12]CPP, 24-crown-8, catenane **B**, and catenane **D** are depicted in Figure 5a, providing insights into the non-covalent interactions between these components in their free and mechanically interlocked states. The proton signals of the outer [12]CPP in the catenane structure [12]CPP exhibited only a minor downfield shift relative to the free [12]CPP. In contrast, the proton signals of 24-crown-8 in catenane **B** shifted upfield by 0.22 ppm compared to free 24-crown-8, reflecting a significant change in the electronic environment of the crown ether upon interlocking with the dibenzylammonium macrocycle. Most strikingly, in catenane **D**, the proton signals of 24-crown-8 showed a pronounced upfield shift of 1.89 ppm compared to free 24-crown-8, which strongly suggests that the 24-crown-8 protons are permanently experiencing the diatropic ring current of the phenylene units in [12]CPP, as would be expected in the mechanically interlocked state.[66] Additionally, the diffusion coefficients of [12]CPP, 24-crown-8, and the dibenzylammonium macrocycle in catenane **D**, which were determined as ca. 3.2×10^{-10} m^2 s^{-1} in diffusion-ordered NMR spectroscopy (DOSY), further support the conclusion that these three components are part of the same molecule (Figure 5b and Figure S8).

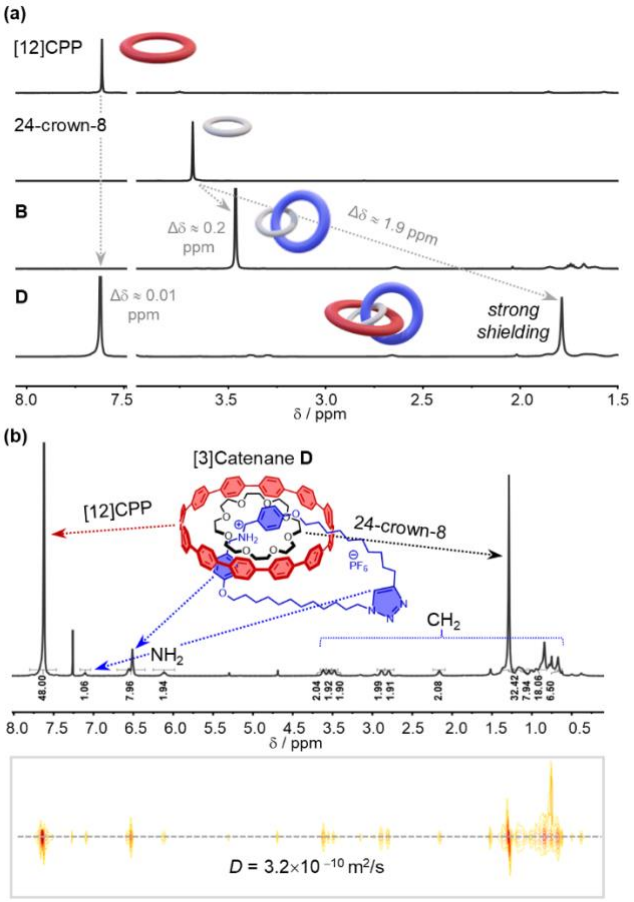

Figure 5. (a) Partial ^{1}H NMR spectra ($CDCl_3$, 500 MHz, 298 K): [12]CPP, 24-crown-8, catenane **B** and catenane **D**. (b) ^{1}H NMR assignments and DOSY NMR characterizations of catenane **D** ($CDCl_3$, 600 MHz, 298 K).

We next investigated the photophysical properties of catenane **D** to assess the impact of incorporating two distinct units into the [12]CPP scaffold (Fgure 6). The maximum absorption of catenane **D** was observed at 344 nm, showing a slight red-shift of 4 nm compared to the parent [12]CPP. However, the absorption band at approximately 450 nm remained unchanged, indicating that the formation of the mechanical bond did not significantly disrupt the symmetry of the ground and excited states of [12]CPP.[67] Catenane **D** exhibited similar fluorescence lifetimes ($\tau \approx 2.7$ ns) as [12]CPP (Figure S9), but the photoluminescence quantum yield (Φ_F) decreased to 70% (compared to 81% for [12]CPP)[68]. This moderate reduction in quantum yield may be attributed to non-radiative relaxation pathways that arise from the proximity of relatively flexible guest molecules.

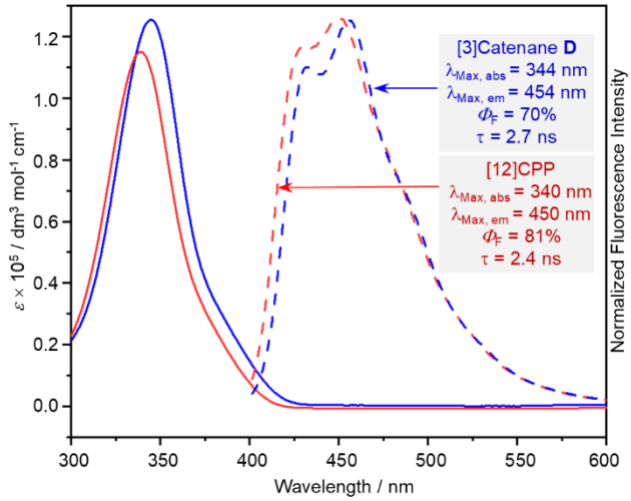

Figure 6. UV-Vis absorbance (solid lines) and fluorescence (dashed lines) spectra for [3]catenane **D** and [12]CPP.

Due to its unusual composition of two flexible rings and one extremely rigid ring, we proceeded to investigate in silico the dynamics of catenane **D**. Specifically, we focused on the rotation, tilting and translation of [12]CPP and 24-crown-8 around the macrocycle. Based on recent studies on similar interlocked structures[51, 69] and supramolecular polymers[70-72], we combined classic molecular dynamics (MD) and well-tempered metadynamics (WT-MetaD)[73,74] to characterize the motion of this catenane. The atomistic model, shown in Figure 7, was built and parametrized according to the GAFF force-field[75]. The catenane model was immersed in a simulation box with explicit chloroform and PF_6^- counterions. After initial energy minimization, the system was equilibrated under NPT conditions at 298 K (see Methods section in the SI for complete details of models and simulations).

As a first step, we examined the kinetics of the CPP nanohoop (Figure 7: in red) unbinding from the 24-crown-8 (in black). We performed multiple replicas of infrequent WT-MetaD simulations allowing to estimate a characteristic CPP unbinding time of ca.10 μs, corresponding to a kinetic barrier of 10.5 ± 0.3 kcal mol^{-1} (estimated from the unbinding timescale via Eyring equation). Extending this approach to explore the kinetics of unbinding of the crown ether (Figure 7: in black) from the protonated station/site of the macrocycle (in blue), we could observe a characteristic unbinding time of ~120 μs (corresponding to

a barrier of ~11.8 ± 0.3 kcal mol^{-1}). This indicates that the diffusion of the black ring along the blue thread macrocycle is at least one order of

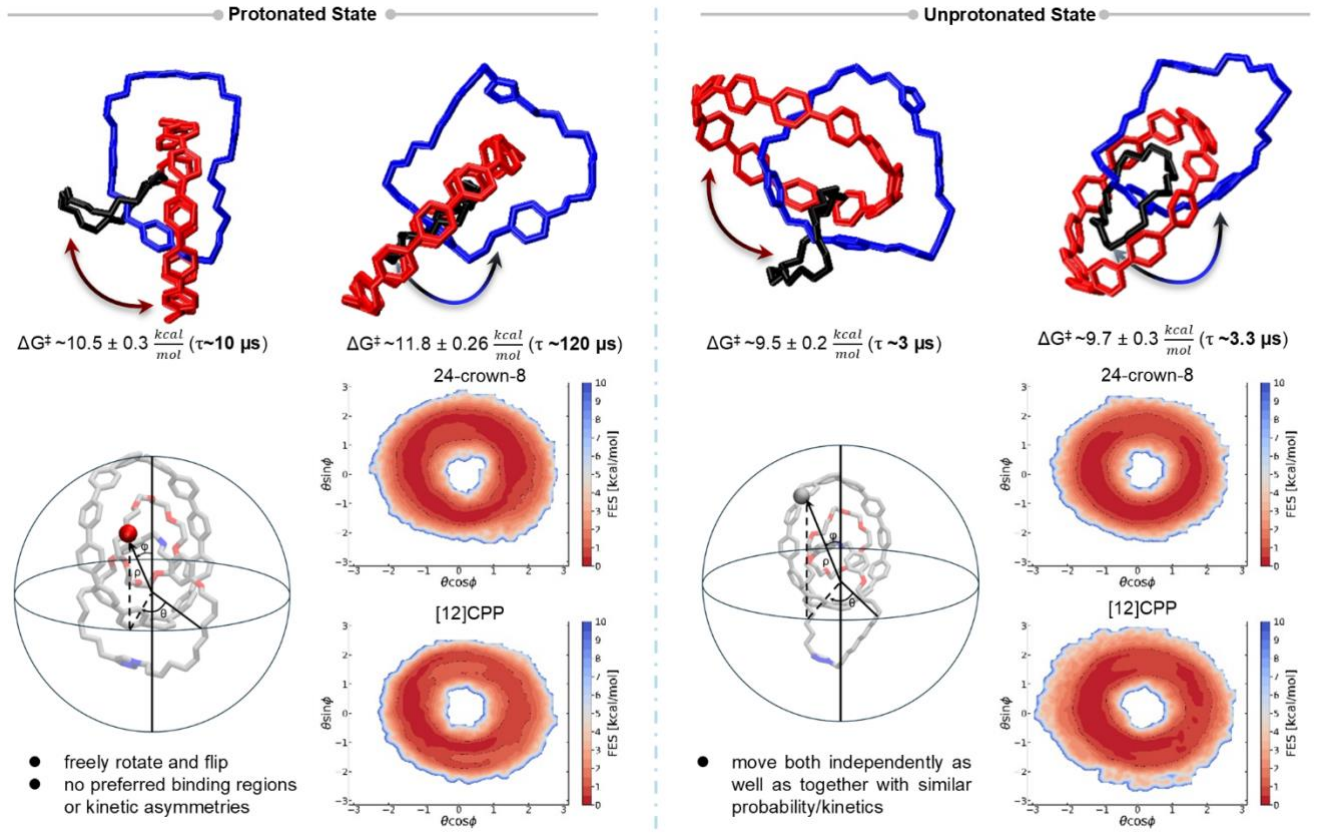

Figure 7. Dynamics of [3]catenane in the protonated (left) and unprotonated (right) state. The top panels illustrate the kinetics of [12]CPP and 24-crown-8 unbinding. The bottom panels show the free-energy surfaces for the rotational and tilting motions of the rings.

magnitude slower/less-likely than the separation/unbinding between the two red and black rings: in other words, under these conditions, it is statistically likely to observe the red and black rings diffusing separately and independently from each other along the blue macrocycle thread.

To further characterize the motion of catenane **D**, we performed 200 ns of classic MD simulations, starting from the "bound" configuration. Using a spherical coordinate system, we decomposed the motion of the two rings relative to the macrocycle into the rotational (θ) and tilting (φ) components.[44, 60] The resulting free energy surfaces (Figure 7: bottom row) indicate that both CPP and 24-crown-8 can freely rotate and flip, as no preferred binding regions or kinetic asymmetries can be noticed.

Additionally, we also simulated the dynamical behavior of catenane **D** in basic medium, where the macrocycle is unprotonated. In this state, the estimated CPP-ring/24-crown-8 unbinding time is ~3 μs, corresponding to a barrier of ~9.5 kcal mol^{-1}. In this case, this is found very close to the characteristic activation barrier for the diffusion of the crown ether (in black) along the blue macrocycle thread (in blue): ~9.7 kcal mol^{-1}, corresponding to a characteristic escape time from the (unprotonated, in these conditions) binding station of ~3.3 μs. This indicates that, under basic conditions, the interaction between the red and black rings is comparable to that between the black ring and the blue thread. In contrast to the protonated case, where the electrostatic interaction between the blue and black rings is dominant, this thus depicts a scenario where the two rings can move both independently as well as together with similar probability/kinetics. This suggests the presence of residual non-specific interactions between the black and the blue ring even in the absence of protonation, as, in a hypothetical case where the blue-black interaction is negligible compared to the red-black interaction, the red and black rings would diffuse along the blue thread macrocycle preferentially together. These results also demonstrate the remarkable effects that changing the surrounding conditions may have in determining and modifying the internal dynamics of such interlocked systems.

CONCLUSIONS

We have successfully synthesized a rare ABC-type hetero[3]catenane using a ring-in-ring assembly strategy, incorporating unaltered [12]CPP, 24-crown-8 and a dibenzylammonium macrocycle. X-ray crystal structure analysis revealed the key assembly properties of the binary

[12]CPP⊃24-crown-8 and ternary [12]CPP⊃24-crown-8⊃**9** complexes. The formation of the mechanical bond was confirmed through several complementary methods, including tandem mass spectrometry. CID studies helped to rule out non-covalent adducts and indicated that macrocycle **A** is the weakest link in hetero[3]catenane **D**. The photophysical properties of catenane **D** showed that the introduction of flexible macrocycles had a modest effect on the absorption and fluorescence properties of [12]CPP. Molecular simulations provided insights on the internal dynamics of the catenane and showed that the larger CPP ring can slip across the smaller crown ether ring. Estimating barriers and characteristic timescales for the motions of all the sub-components of the catenane relative to each other also revealed the key role of the protonation state, which may be used to control and modify the dynamics of the system.

Our findings underscore the promise of the ring-in-ring assembly strategy for creating MIMs with intricate architectures. Moving forward, it should be feasible to extend the approach towards the synthesis of hetero[3]rotaxanes, polyrotaxanes and MIMs with low symmetry and intricate topology.[76] Even functional systems may be prepared such as new pH-controlled ABC-type molecular machines and unique mechanically interlocked, networked polymers.[77, 78]

ASSOCIATED CONTENT

Supporting Information. General experimental details and procedures, X-ray crystallographic details, computational details, ^{1}H NMR spectra, and ^{13}C{^{1}H} NMR spectra.

Data availability. Details on the procedures for the parametrization of the molecular models and on the simulations' setup, along with additional simulation data, are provided in the Methods section and in the ESI file. Complete data and materials pertaining to the molecular simulations conducted herein (input files, model files, raw data, analysis, *etc.*) are available at: https://github.com/luigileanza/CPP-3-catenanes (this temporary folder will be replaced by a DOI Zenodo archive upon acceptance of the definitive version of this paper). Other information needed is available from the corresponding author upon reasonable request.

AUTHOR INFORMATION

Corresponding Author

Youzhi Xu – College of Chemistry and Molecular Sciences, Henan University, Kaifeng 475004, China. E-mail: youzhixu@henu.edu.cn

Giovanni M. Pavan – Department of Applied Science and Technology, Politecnico di Torino, Corso Duca degli Abruzzi, 24, 10129 Torino, Italy. E-mail: giovanni.pavan@polito.it

Max von Delius – Institute of Organic Chemistry, Ulm University, Albert-Einstein-Allee 11, 89081 Ulm, Germany. E-mail: max.vondelius@uni-ulm.de

Pingwu Du – Hefei National Laboratory for Physical Sciences at the Microscale, CAS Key Laboratory of Materials for Energy Conversion, Department of Materials Science and Engineering, University of Science and Technology of China, Hefei, Anhui Province, 230026 China. E-mail: dupingwu@ustc.edu.cn

ACKNOWLEDGMENT

Y.X. and P.D. acknowledge funding from the National Natural Science Foundation of China (22201064, 22471060 and 22225108) and The Joint Fund of Henan Provincial Science and Technology Research and Development Plan (235200810074). M.v.D. acknowledges financial support by the Deutsche Forschungsgemeinschaft (DFG) under project numbers 182849149 (SFB953 "Synthetic Carbon Allotropes", projectA7) and 364549901 (SFB TRR 234 "Cata-Light", project B7).

REFERENCES

1. Mena-Hernando, S.; Pérez, E. M. Mechanically Interlocked Materials. Rotaxanes and Catenanes Beyond the Small Molecule. *Chem. Soc. Rev.* **2019**, *48*, 5016–5032.
2. Saura-Sanmartin, A.; Schalley, C. A. Self-Sorting as a Versatile Strategy in the Synthesis of Rotaxanes and Catenanes. Chem **2023**, *9*, 823–846.
3. Erbas-Cakmak, S.; Leigh, D. A.; McTernan, C. T.; Nussbaumer, A. L. Artificial Molecular Machines. *Chem. Rev.* **2015**, *115*, 10081–10206.
4. Kench, T.; Summers, P. A.; Kuimova, M. K.; Lewis, J. E. M.; Vilar, R. Rotaxanes as Cages to Control DNA Binding, Cytotoxicity, and Cellular Uptake of a Small Molecule. *Angew. Chem. Int. Ed.* **2021**, *60*, 10928–10934.
5. Mo, X.; Deng, Y.; Lai, S. K.-M.; Gao, X.; Yu, H.-L.; Low, K.-H.; Guo, Z.; Wu, H.-L.; Au-Yeung H. Y.; Tse, E. C. M. Mechanical Interlocking Enhances the Electrocatalytic Oxygen Reduction Activity and Selectivity of Molecular Copper Complexes. *J. Am. Chem. Soc.* **2023**, *145*, 6087–6099.
6. Heard, A. W.; Goldup, S. M. Synthesis of a Mechanically Planar Chiral Rotaxane Ligand for Enantioselective Catalysis. *Chem* **2020**, *6*, 994–1006.
7. Loeb, S. J. Rotaxanes as Ligands: from Molecules to Materials. *Chem. Soc. Rev.* **2007**, *36*, 226–235.
8. Goswami, A.; Saha, S.; Biswas, P. K.; Schmittel, M. (Nano)mechanical Motion Triggered by Metal Coordination: from Functional Devices to Networked Multicomponent Catalytic Machinery. *Chem. Rev.*, **2019**, *120*, 125–199.
9. Diederich, F.; Dietrich-Buchecker, C.; Nierengarten, J.-F.; Sauvage, J.-P. A Copper(I)-Complexed Rotaxane with Two Fullerene Stoppers. *J. Chem. Soc. Chem. Commun.* **1995**, 781–782.
10. Lewis, J. E. M.; Beer, P. D.; Loeb, S. J.; Goldup, S. M. *Chem. Soc. Rev.* Metal Ions in the Synthesis of Interlocked Molecules and Materials. **2017**, *46*, 2577–2591.
11. Wu, Q.; Rauscher, P. M.; Lang, X.; Wojtecki, R. J.; Pablo, J. J. d.; Hore, M. J. A.; Rowan, S. J. Poly[n]catenanes: Synthesis of Molecular Interlocked Chains. *Science* **2017**, *358*, 1434–1439.
12. Oka, Y.; Masai, H.; Terao, J. Multistate Structural Switching of [3]Catenanes with Cyclic Porphyrin Dimers by Complexation with Amine Ligands. *Angew. Chem. Int. Ed.* **2023**, *62*, e202217002.
13. Yang, S.; Zhao, C.-X.; Crespi, S.; Li, X.; Zhang, Q.; Zhang, Z.-Y.; Mei, J.; Tian, H.; Qu, D.-H. Reversibly Modulating a Conformation Adaptive Fluorophore in [2]Catenane. *Chem* **2021**, *7,* 1544–1556.
14. Fujimura, K.; Ueda, Y.; Yamaoka, Y.; Takasu, K.; Kawabata, T.; Rotaxane Synthesis by an End-Capping Strategy via Swelling Axle-Phenols. *Angew. Chem. Int. Ed.* **2023**, *62,* e202303078.
15. Pearce, N.; Reynolds, K. E. A.; Kayal, S.; Sun, X. Z.; Davies, E. S.; Malagreca, F.; Schürmann, C. J.; Ito, S.; Yamano, A.; Argent, S. P.; George, M. W.; Champness, N. R. Selective Photoinduced Charge Separation in Perylenediimide-pillar[5]arene Rotaxanes. *Nat. Commun.* **2022**, *13,* 415.

16. Spruell, J. M.; Coskun, A.; Friedman, D. C.; Forgan, R. S.; Sarjeant, A. A.; Trabolsi, A.; Fahrenbach, A. C.; Barin, G.; Paxton, W. F.; Dey, S. K.; Olson, M. A.; Benítez, D.; Tkatchouk, E.; Colvin, M. T.; Carmielli, R.; Caldwell, S. T.; Rosair, G. M.; Hewage, S. G.; Duclairoir, F.; Seymour, J. L.; Slawin, A. M. Z.; Goddard, W. A.; Wasielewski, M. R.; Cooke. G.; Stoddart, J. F. Highly Stable Tetrathiafulvalene Radical Dimers in [3]Catenanes. *Nat. Chem.* **2010**, *2*, 870–879.
17. Dasgupta, S.; Wu, J. Formation of [2]Rotaxanes by Encircling [20], [21] and [22]Crown Ethers onto the Dibenzylammonium Dumbbell. *Chem. Sci.* **2012**, *3*, 425–432.
18. Thibeault, D.; Morin, J.-F. Recent Advances in the Synthesis of Ammonium-Based Rotaxanes. *Molecules*, **2010**, *15,* 3709–3730.
19. Zhang, Z.; Zhao, J.; Yan, X. *Acc. Chem. Res.* **2024**, *57*, 992–1006.
20. Xia, D.; Wang, P.; Ji, X.; Khashab, N. M.; Sessler, J. L.; Huang, F. Functional Supramolecular Polymeric Networks: The Marriage of Covalent Polymers and Macrocycle-Based Host–Guest Interactions. *Chem. Rev.* **2020**, *120,* 6070–6123.
21. Kato, K.; Fa, S.; Ohtani, S.; Shi, T.-h.; Brouwer, A. M.; Ogoshi, T. Noncovalently Bound and Mechanically Interlocked Systems Using Pillar[n]arenes. *Chem. Soc. Rev.* **2022,** *51,* 3648–3687.
22. Chen, L.; Nixon, R.; De Bo, G. Force-Controlled Release of Small Molecules with a Rotaxane Actuator. *Nature* **2024**, *628,* 320-325.
23. Wang, X. Q.; Li, W. J.; Wang, W.; Yang, H. B. Rotaxane Dendrimers: Alliance between Giants. *Acc. Chem. Res.* **2021**, *54,* 4091–4106.
24. Zheng, X.; Zhang, Y.; Cao, N.; Li, X.; Zhang, S.; Du, R.; Wang, H.; Ye, Z.; Wang, Y.; Cao, F.; Li, H.; Hong, X.; Sue, A. C. H.; Yang, C.; Liu, W.-G.; Li, H. Coulombic-Enhanced Hetero Radical Pairing Interactions. *Nat. Commun.* **2018**, ***9,*** 1961.
25. Odell, B.; Reddington, M. V.; Slawin, A. M. Z.; Spencer, N.; Stoddart, J. F.; Williams, D. J. Cyclobis(paraquat-p-phenylene). A Tetracationic Multipurpose Receptor. *Angew. Chem. Int. Ed. Engl.* **1988**, *27*, 1547–1550.
26. Cai, K.; Lipke, M. C.; Liu, Z.; Nelson, J.; Cheng, T.; Shi, Y.; Cheng, C.; Shen, D.; Han, J.-M.; Vemuri, S.; Feng, Y.; Stern, C. L.; Goddard, W. A.; Wasielewski, M. R. Stoddart, J. F. Molecular Russian Dolls. *Nat. Commun.* **2018**, *9.* 5275.
27. Schill, G.; Lüttringhaus, A. The Preparation of Catena Compounds by Directed Synthesis. *Angew. Chem. Int. Ed.* **1964**, *3,* 546–547.
28. Chen, Q.; Zhu, K. Advancements and Strategic Approaches in Catenane Synthesis. *Chem. Soc. Rev.* **2024**, *53*, 5677–5703
29. Gil-Ramírez, G.; Leigh, D. A.; Stephens, A. J. Catenanes: Fifty Years of Molecular Links. *Angew. Chem. Int. Ed.* **2015** *54*, 6110–6150
30. Evans N. H.; Beer, P. D. Progress in the Synthesis and Exploitation of Catenanes Since the Millennium. *Chem. Soc. Rev.* **2014**, *43*, 4658–4683.
31. Zhang, L.; Qiu, Y.; Liu, W.-G.; Chen, H.; Shen, D.; Song, B.; Cai, K.; Wu, H.; Jiao, Y.; Feng, Y.; Seale, J. S. W.; Pezzato, C.; Tian, J.; Tan, Y.; Chen, X.-Y.; Guo Q.-H.; Stern, C. L.; Philp, D.; Astumian, R. D.; Goddard, W. A. III; Stoddart, J. F. An Electric Molecular Motor. *Nature* **2023**, *613*, 280–286.
32. Leigh, D. A.; Wong, J. K.; Dehez, F.; Zerbetto, F. Unidirectional Rotation in a Mechanically Interlocked Molecular Rotor. *Nature* **2003**, *424*,174–179.
33. Erbas-Cakmak, S.; Fielden, S. D. P.; Karaca, U.; Leigh, D. A. McTernan, C. T.; Tetlow, D. J.; Wilson, M. R. Rotary and Linear Molecular Motors Driven by Pulses of a Chemical Fuel. *Science* **2017**, *358*, 340–343.
34. Amabilino, D. B.; Ashton, P. R.; Reder, A. S.; Spencer, N.; Stoddart, J. F. Olympiadane. *Angew. Chem. Int. Ed. Engl.* **1994**, *33*, 1286–1290.
35. Ng A. W. H.; Yee. C. C.; Au-Yeung, H. Y. Radial Hetero[5]catenanes: Peripheral Isomer Sequences of the Interlocked Macrocycles. *Angew. Chem. Int. Ed.* **2019**, *58*, 17375–17382.
36. Podh M. B.; Ratha, R.; Purohit, C. S. Template Assisted Synthesis of Linear [5]Catenane by Post-Functionalization of Templated [2]Catenane and Using Click Reaction. *Chem. Asian J.* **2024**, *19*, e202400351.
37 Megiatto, J. D. Jr.; Schuster, D. I. "Click" Methodology for Synthesis of Functionalized [3]Catenanes: Toward Higher Interlocked Structures. *Chem. Eur. J.* **2009**, *15*, 5444–5448.
38 Ng, A. W. H.; Lai, S. K.; Yee, C. C.; Au-Yeung, H. Y. Macrocycle Dynamics in a Branched [8]Catenane Controlled by Three Different Stimuli in Three Different Regions. *Angew. Chem. Int. Ed.* **2022**, *61*, e202110200.
39. Golder, M. R.; Jasti, R. Syntheses of the Smallest Carbon Nanohoops and the Emergence of Unique Physical Phenomena. *Acc. Chem. Res.* **2015**, *48,* 557–566.
40. Jasti, R.; Bhattacharjee, J. Neaton, J. B.; Bertozzi, C. R. Synthesis, Characterization, and Theory of [9]-, [12]-, and [18]Cycloparaphenylene: Carbon Nanohoop Structures. *J. Am. Chem. Soc.* **2008**, *130,* 17646–17647.
41. Takaba, H.; Omachi, H.; Yamamoto, Y.; Bouffard, J.; Itami, K. Selective Synthesis of [12]Cycloparaphenylene. *Angew. Chem. Int. Ed.* **2009**, *48,* 6112–6116.
42. Yamago, S.; Watanabe, Y.; Iwamoto, T. Synthesis of [8]Cycloparaphenylene from a Square-Shaped Tetranuclear Platinum Complex. *Angew. Chem. Int. Ed.* **2010**, *49,* 757–759.
43. Omachi, H.; Nakayama, T.; Takahashi, E.; Segawa, Y.; Itami, K. Initiation of Carbon Nanotube Growth by Well-Defined Carbon Nanorings. *Nat. Chem.* **2013**, *5*, 572–576.
44. Xu, Y.; von Delius, M. The Supramolecular Chemistry of Strained Carbon Nanohoops. *Angew. Chem. Int. Ed.* **2020**, *59,* 559–573.
45. Chang, X.; Xu, Y.; von Delius, M. Recent Advances in Supramolecular Fullerene Chemistry. *Chem. Soc. Rev.* **2024**, *53,* 47–83.
46. Sacristán-Martín, A.; Schwer, F.; Pickl, T.; Lebzelter, A.; Pöthig, A.; von Delius, M. A Chiral Nanohoop as Highly Efficient Asymmetric Organocatalyst. *ChemRXiv* **2024**, DOI: 10.26434/chemrxiv-2024-srqv5-v2.
47. Leonhardt, E. J.; Jasti, R. Emerging Applications of Carbon Nanohoops. *Nat. Rev. Chem.* **2019**, *3*, 672–686.
48. Hermann, M.; Wassy, D.; Esser, B. Conjugated Nanohoops Incorporating Donor, Acceptor, Hetero- or Polycyclic Aromatics. *Angew. Chem. Int. Ed.* **2021**, *60*, 15743–15766.
49. Schwer, F.; Zank, S.; Freiberger, M.; Steudel, F. M.; Geue, N.; Ye, L.; Barran, P. E.; Drewello, T.; Guldi, D. M.; von Delius, M. Nanohoops Favour Light-Induced Energy Transfer over Charge Separation in Porphyrin/[10]CPP/Fullerene Rotaxanes. *Angew. Chem. Int. Ed.* **2024**, *63*, e202413404
50. Xu, Y.; Kaur, R.; Wang, B.; Minameyer, M. B.; Gsänger, S.; Meyer, B.; Drewello, T.; Guldi, D. M.; von Delius, M. Concave–Convex π–π Template Approach Enables the Synthesis of [10]Cycloparaphenylene–Fullerene [2]Rotaxanes. *J. Am. Chem. Soc.* **2018**, *140*, 13413–13420.
51. Steudel, F. M.; Ubasart, E.; Leanza, L.; Pujals, M.; Parella, T.; Pavan, G. M.; Ribas, X.; von Delius, M. Synthesis of C60/[10]CPP-Catenanes by Regioselective, Nanocapsule-Templated Bingel Bis-Addition. *Angew. Chem. Int. Ed.* **2023**, *62,* e202309393.
52. May, J. H.; Van Raden, J. M.; Maust, R. L.; Zakharov, L. N.; Jasti, R. Active Template Strategy for the Preparation of π-Conjugated Interlocked Nanocarbons. *Nat. Chem.* **2023**, *15,* 170–176.
53. May, J. H.; Fehr, J. M.; Lorenz, J. C.; Zakharov, L. N.; Jasti, R. A High-Yielding Active Template Click Reaction (AT-CuAAC) for the Synthesis of Mechanically Interlocked Nanohoops. *Angew. Chem. Int. Ed.* **2024**, *63,* e202401823.
54. Fan, Y.-Y.; Chen, D.; Huang, Z.-A.; Zhu, J.; Tung, C.-H.; Wu, L.-Z.; Cong, H. An Isolable Catenane Consisting of Two Möbius Conjugated Nanohoops. *Nat. Commun.* **2018,** *9*, 3037.
55. Van Raden, J. M.; White, B. M.; Zakharov, L. N.; Jasti, R.

Nanohoop Rotaxanes from Active Metal Template Syntheses and Their Potential in Sensing Applications. *Angew. Chem. Int. Ed.* **2019**, *58,* 7341–7345.
56. Ishibashi, H.; Rondelli, M.; Shudo, H.; Maekawa, T.; Ito, H.; Mizukami, K.; Kimizuka, N.; Yagi, A.; Itami, K. Noncovalent Modification of Cycloparaphenylene by Catenane Formation Using an Active Metal Template Strategy. *Angew. Chem. Int. Ed.* **2023**, *62,* e202310613.
57. Bu, A.; Gao, J. N.; Chen, Y.; Xiao, H.; Li, H.; Tung, C. H.; Wu, L.-Z.; Cong, H. Modular Synthesis of Improbable Rotaxanes with All-Benzene Scaffolds. *Angew. Chem. Int. Ed.* **2024**, *63,* e202401838.
58. Segawa, Y.; Kuwayama, M.; Hijikata, Y.; Fushimi, M.; Nishihara, T.; Pirillo, J.; Shirasaki, J.; Kubota, N.; Itami, K. Topological Molecular Nanocarbons: All-Benzene Catenane and Trefoil Knot. *Science* **2019**, 276, 272–276.
59. Bu, A.; Zhao, Y.; Xiao, H.; Tung, C. H.; Wu L.-Z.; Cong, H. A Conjugated Covalent Template Strategy for All-Benzene Catenane Synthesis. *Angew. Chem. Int. Ed.* **2022**, *61,* e202209449.
60. Narita, N.; Kurita, Y.; Osakada, K.; Ide, T.; Kawai, H.; Tsuchido, Y. A Dodecamethoxy[6]cycloparaphenylene Consisting Entirely of Hydroquinone Ethers: Unveiling in-plane Aromaticity Through a Rotaxane Structure. *Nat. Commun.* **2023**, *14,* 8091.
61. Fan, Y.; He, J.; Liu, L.; Liu, G.; Guo, S.; Lian, Z.; Li, X.; Guo, W.; Chen, X.; Wang, Y.; Jiang, H. Chiral Carbon Nanorings: Synthesis, Properties and Hierarchical Self-assembly of Chiral Ternary Complexes Featuring a Narcissistic Chiral Self-Recognition for Chiral Amines. *Angew. Chem. Int. Ed.* **2023**, *62,* e202304623.
62. Zhu, K.; Baggi, G.; Loeb, S. J. Ring-Through-Ring Molecular Shuttling in a Saturated [3]Rotaxane. *Nat. Chem.* **2018**, *10*, 625–630.
63. Grabicki, N.; Nguyen, K. T. D.; Weidner, S.; Dumele, O. Confined Spaces in [n]Cyclo-2,7-pyrenylenes. *Angew. Chem. Int. Ed.* **2021**, *60,* 14909–14914.
64. Fan, Y,; He, J,; Guo, S.; Jiang, H. Host-Guest Chemistry in Binary and Ternary Complexes Utilizing π-Conjugated Carbon Nanorings. *ChemPlusChem* **2024**, *89*, e202300536.
65. Ubasart, E.; Borodin, O.; Fuertes-Espinosa, C.; Xu, Y.; García-Simón, C.; Gómez, L.; Juanhuix, J.; Gándara, F.; Imaz, I.; von Delius, M.; Ribas, X. A Three-Shell Supramolecular Complex Enables the Symmetry-Mismatched Chemo- and Regioselective Bis-Functionalization of C_{60}. *Nat. Chem.* **2021**, *13*, 420–427.
66. Gregolińska, H.; Majewski, M.; Chmielewski, P. J.; Gregoliński, J.; Chien, A.; Zhou, J.; Wu, Y.-L.; Bae, Y. J.; Wasielewski, M. R.; Zimmerman, P. M.; Stępień, M. Fully Conjugated [4]Chrysaorene. Redox-Coupled Anion Binding in a Tetraradicaloid Macrocycle. *J. Am. Chem. Soc.* **2018,** *140*, 14474–14480.
67. Darzi, E. R.; Jasti, R. The Dynamic Size-Dependent Properties of [5]-[12]Cycloparaphenylenes. *Chem. Soc. Rev.* **2015**, *44*, 6401–6410.
68. Sisto, T. J.; Golder, M. R.; Hirst, E. S.; Jasti, R. Selective Synthesis of Strained [7]Cycloparaphenylene: An Orange-Emitting Fluorophore. *J. Am. Chem. Soc.* **2011**, *133*, 15800-15802.
69. Leanza, L.; Perego, C.; Pesce, L.; Salvalaglio, M.; von Delius, M.; Pavan. G. M. Into the Dynamics of Rotaxanes at Atomistic Resolution. *Chem. Sci.* **2023**, *14*, 6716–6729.
70. Bochicchio, D.; Salvalaglio, M.; Pavan, G. M. Into the Dynamics of a Supramolecular Polymer at Submolecular Resolution. *Nat. Commun.* **2017**, *8*, 147.
71. de Marco, A. L.; Bochicchio, D.; Gardin, A.; Doni, G.; Pavan, G. M. Controlling Exchange Pathways in Dynamic Supramolecular Polymers by Controlling Defects. *ACS Nano* **2021**, *15*, 14229–14241.
72. Weyandt, E.; Leanza, L.; Capelli, R.; Pavan, G. M.; Vantomme, G.; Meijer, E. W. Controlling the Length of Porphyrin Supramolecular Polymers via Coupled Equilibria and Dilutioninduced Supramolecular polymerization. *Nat. Comm*. **2022**, *13*, 248.
73. Tiwary, P.; Parrinello, M. From Metadynamics to Dynamics. *Phys. Rev. Lett.* **2013**, *111*, 230602.
74. Barducci, A.; Bussi, G.; Parrinello, M. Well-Tempered Metadynamics: A Smoothly Converging and Tunable Free-Energy Method. *Phys. Rev. Lett*. **2008**, *100*, 020603.
75. Wang, J.; Wolf, R. M.; Caldwell, J. W.; Kollman, P. A.; Case, D. A. Development and Testing of a General Amber Force Field. *J. Comput. Chem.* **2004**, *25*, 1157–1174.
76. Bruns, C. J.; Stoddart, J. F. The Nature of the Mechanical Bond; John Wiley & Sons, Inc.: Hoboken, NJ, 2016.
77. Xu, W.-T.; Wang, W. Cycloparaphenylene-based [2]Catenanes: Interlocking the Carbon Nanohoops. *Org. Chem. Front.* **2024**, *11*, 1490–1494.
78. Roy, R.; Brouillac, C.; Jacques, E.; Quinton, C.; Poriel, C. π-Conjugated Nanohoops: A New Generation of Curved Materials for Organic Electronics. *Angew. Chem. Int. Ed.* **2024**, *63*, e202402608.

Insert Table of Contents artwork here